*Int. J. Electrochem. Sci.*, 8 **(2013)** 6722 - 6733

International Journal of
ELECTROCHEMICAL
SCIENCE
www.electrochemsci.org

# Effect of Triton X-100 as Dispersant on Carbon Black for $LiFePO_4$ Cathode

*Zhian Zhang, Changming Qu, Tao Zheng, Yanqing Lai, Jie Li*[*]

School of Metallurgical Science and Engineering, Central South University, Changsha 410083, China
[*]E-mail: csulijie@126.com

*Received:* 8 March 2013 / *Accepted:* 3 April 2013 / *Published:* 1 May 2013

In this paper, the poly (ethylene glycol) p-isooctyl-phenyl ether (Triton X-100) as a dispersant is used to pre-disperse the nano-carbon black (SP) in organic N-methyl-pyrrolidone (NMP) solvent. This pre-dispersed carbon black (SP-T) as conductive agent is applied to $LiFePO_4$ cathodes. The dispersion property of nano-carbon black with/without Triton X-100 is evaluated using laser granulometry measurements and rheology test. The $LiFePO_4$ cathodes with pre-dispersed carbon black (SP-T) are examined by scanning electron microscopy (SEM), cyclic voltammograms (CV), electrochemical impendence spectroscopy (EIS) and charge/discharge cycling performance test compared with the $LiFePO_4$ cathode with SP. Results show that the $LiFePO_4$ cathodes with SP-T exhibit improved rate behavior and better cycle performance than the $LiFePO_4$ cathode with SP. The $LiFePO_4$/SP-T cathode containing 1.5 wt.% of Triton X-100 presents the best electrochemical property, exhibiting discharge capacity of 123.9 mAh $g^{-1}$ after 200 cycles at 1C (93.9% capacity retention) and 101.0 mAh $g^{-1}$ at 4 C. Because pre-dispersed carbon black (SP-T) is dispersed homogeneously in the dried composite electrode to form a better electronic wiring of the active material particles, so as to enhance electrochemical performance of the cathodes.

**Keywords:** $LiFePO_4$ cathode, carbon black, Triton X-100, dispersion.

## 1. INTRODUCTION

Lithium ion battery based on $LiFePO_4$ cathode has been considered as one of the most promising candidates for large-scale application in electric vehicle, hybrid electric vehicle and smart grid due to its excellent chemical and thermal stability, good safety, low toxicity and low cost [1-2]. Among the components in the $LiFePO_4$ cathode, the conductive agent plays an important role in improving cell performance, especially in regards to cycle life [3-4].

The conductive carbon materials which have good conductivity and electrochemical stability are widely used as a conductive agent in lithium ion battery, especially nano-conductive carbon additives, such as acetylene black (AB), Ketjen black (KB), Super P (SP) and carbon nanotubes. However, it is really difficult to make these kinds of nano-conductive carbon particles disperse homogeneously into the slurry because they have a tendency to flocculate due to their large surface area and high oil adsorption, especially when the particulates must be dispersed in highly dense suspensions of active materials. [5-8] If the conductive particulates are dispersed heterogeneously in the cathode, not only might the performances of the battery deteriorate, but also production speed, yield and battery safety could be affect [9].

To overcome this problem, dispersing carbon black before the slurry preparation has been considered a way to form more homogeneous carbon black distribution within the dried composite electrode, which could reduce internal resistance and enhance electrochemical performance of cathode materials [9-10]. Chemical dispersants can be adsorbed on the surface of the nano-particles, and prevent the particles from agglomerating through electrostatic repulsion or steric effects, thus forming well-dispersed suspension of nanoparticles [11]. Carbon black can be dispersed by chemical dispersant in organic medium. Recently, two carboxylic dispersants (EACH, CP) are applied to disperse carbon black in organic medium, which result in a decrease of powder aggregation and the suspension viscosity [12]. Tomlinson et al. [13] research on commercial succinimide as a dispersant for carbonaceous solid substrates in hydrocarbon solvents. Matthew et al. [14] reported three different dispersants surround carbon black particles and form a colloidal suspension. Moreover, orotan® is an effective dispersant (polyacrylate dispersant) for dispersing carbon black in distilled water. [15]

However, the application of dispersants for the lithium-ion battery is few, especially for improvement of carbon black particles dispersion in the dried composite electrode, very little work has been reported. Triton X-100 was observed to positively affect the dispersion of carbon black for the aqueous processing of $LiFePO_4$ composite electrodes [16]. But, it is really difficult to completely remove the moisture remained in the electrode [17]. Chang et al. reported conductive carbon can be dispersed by HSC-03 in NMP solvent for $LiFePO_4$ cathode [18].

In this work, poly (ethylene glycol) p-isooctyl-phenyl ether (Triton X-100) is used to pre-disperse the nano-carbon black (SP), which is used commonly in commercial lithium ion batteries as conductive additive, in organic N-methyl-pyrrolidone (NMP) solvent, because NMP is a most common industrial organic solvent-based system in battery manufacture. This pre-dispersed carbon black (SP-T) as conductive agent is applied to $LiFePO_4$ cathodes. We investigate the physical properties of undispersed SP and pre-dispersed SP, respectively, and study effects of different SP on the performance of $LiFePO_4$ cathodes for lithium ion batteries. The dispersion properties of SP are characterized through particle size distribution analysis, scanning electron microscopy and rheology. The charge/discharge cycling performance, electrochemical redox behavior and impendence of $LiFePO_4$ cathodes with pre-dispersed or undispersed SP are examined by using a coin-type cell.

## 2. EXPERIMENTAL

### *2.1 Materials and process*

The commercial carbon-coated $LiFePO_4$ powders with detailed specifications as follows: carbon content (2 wt. %), average particle size (1.3 μm), tap density (1.35 $g \cdot cm^{-3}$) and BET specific surface area (13.7 $m^2 \cdot g^{-1}$). Super P with an average particle size of 40 nm was acquired from TIMCAL Graphite & Carbon, Switzerland. Triton X-100 (Aldrich) $M_{Triton\ X\text{-}100}$ = 652 g $mol^{-1}$ was purchased from Sigma-Aldrich. PVDF (HSV900, Mw=1,000,000) was supplied by Arkema, France.

Pre-dispersion of carbon black: The saturated adsorption amount of Triton X-100 on the SP surface is the ratio of SP and Triton X-100 for 5:1 through theoretical calculation [19]. Here, the study to evaluate the more efficient dispersant by optimizing parameters of the mass ratio of SP and Triton X-100, so we designed the parameters of the mass ratio of SP and Triton X-100 for 10: 1, 20: 3, 5: 1 and 4: 1, respectively. Pre-dispersed suspensions of carbon black were prepared by slowly adding the required amount of dry SP powder to N-methyl-pyrrolidone (NMP, Merck) with/without a dispersing agent (Triton X-100). These materials were mixed by a Polytron PT 10-35 homogenizer at 20000 rpm for 10 min until uniform. The forgoing procedure produce two types of suspensions that SP without Triton X-100 and SP with the Triton X-100 dispersant. The two suspensions of carbon black with different dispersion properties were named as SP and SP-T respectively and used as conductive agent in the following articles.

Preparation of composite electrodes: $LiFePO_4$ and PVDF were added to the two conductive agent paste (SP: PVDF: $LiFePO_4$ is 1:1:8), which Triton X-100 concentrations corresponds to 0, 1, 1.5, 2, 2.5 wt.% in the dried electrodes. The mixing process was performed in a Polytron PT 10-35 homogenizer at 20000 rpm for 20 min until uniform. The mixed slurry was coated onto aluminum foil and dried at 110 °C under vacuum for 24 h to remove the residual solvent. Experience procedure is shown in Fig. 1.

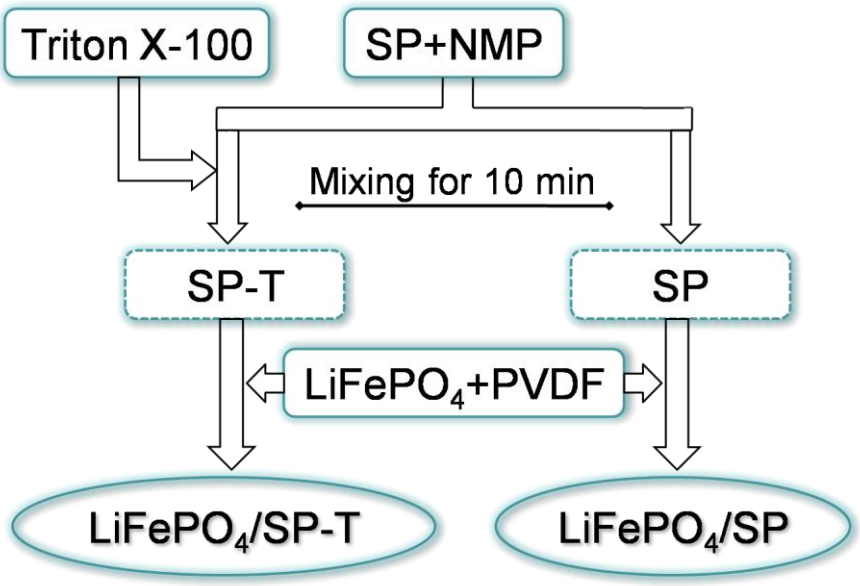


**Figure 1.** Experiment procedure

*2.2 Characterization of the suspensions*

Particles size distribution in dilute medium was measured by low angle laser light scattering using a Mastersizer S laser granulometer (Malvern). A drop of SP/SP-T suspension was diluted in 100 mL of NMP before measurement. The rheological behavior of the SP / SP-T suspension was determined at 25 ℃ using a controlled-stress rheometer (AR1000, TA Instruments Ltd., UK) with a 50 mm diameter plane-and-plane geometry. The classical solvent trap accessory was used to prevent the sample from drying during the measurement. Before the measurement, the sample was need to pre-shear at the rate 1000 $s^{-1}$ for 60 s, and then to let it rest for 600 s. It ensures that all samples have the same mechanical history. Viscosity or shear stress was then measured as a function of the shear rate from 1000 to 0.1 $s^{-1}$ to determine viscosity.

*2.3 Characterization of the electrodes*

Morphology of the electrodes was conducted by SEM (Quanta-200, FEI). The electrochemical performances of the $LiFePO_4$ cathodes were evaluated in CR2025-size button $LiFePO_4$/Li half cells, which were assembled by using Celgard® 2400 membrane as the separator and filled with 85 μL of liquid electrolyte. The lithium electrode in this half cell was used as the counter electrode as well as the reference electrode and the electrolyte was 1 mol/L $LiPF_6$ dissolved in EC/DMC/EMC 1:1:1 by mass co-solvent, which was purchased from Zhangjiagang Guotai-Huarong New Chemical Materials Co., Ltd.,China. All the cells were assembled in an argon-filled glove box (Universal 2440/750, Mikrouna Mech. Tech. Co., Ltd., water content: <1 ppm, oxygen content: <1 ppm).

The cyclic voltammograms (CV) and electrochemical impedance spectra (EIS) of the half cells were measured by using PARSTAT 2273 electrochemical measurement system (PerkinElmer Instrument. USA). CV test was performed at a scan rate of 0.1 $mV \cdot s^{-1}$. For the EIS test, the frequency window was between 1 MHz and 0.01 Hz, with amplitude of 5 mV. The obtained EISs were fitted by using ZView software (Scribner and Associates). The charge-discharge performances were tested between 2.5 V and 4.2 V (vs. $Li/Li^+$) at different rates on a Land charge/discharge instrument.

## 3. RESULTS AND DISCUSSION

*3.1 Study of composite electrode*

Fig. 2 presents cycle performance of $LiFePO_4$/SP-T cathodes with different Triton X-100 contents and $LiFePO_4$/SP cathode at 1 C between 2.5 V and 4.2 V. Comparison of the curves shows that the $LiFePO_4$/SP curve is considerably lower than the $LiFePO_4$/SP-T curves. With concentrations of Triton X-100 increased, the capacity retention ratio of composite electrode is increased firstly then decreased, which Triton X-100 content corresponds to 1.5 wt.% is the best. The discharge capacity of the $LiFePO_4$/SP cathode is 135.2 mAh $g^{-1}$ for the initial cycle and decreases to 116.4 mAh $g^{-1}$ after 200 cycles and the capacity retention ratio is only 83% which is similar to the result reported by Yang et al.

[20] Whereas the discharge capacity of $LiFePO_4$/SP-T cathode (1.5 wt.% of Triton X-100) is 140.2 $mAh \cdot g^{-1}$ for the initial cycle and a high reversible capacity of 127.9 $mAh \cdot g^{-1}$ is retained after 200 cycles with the capacity retention ratio of 93.9%. These results confirm that the $LiFePO_4$/SP-T cathode showing a great improvement in cyclability.

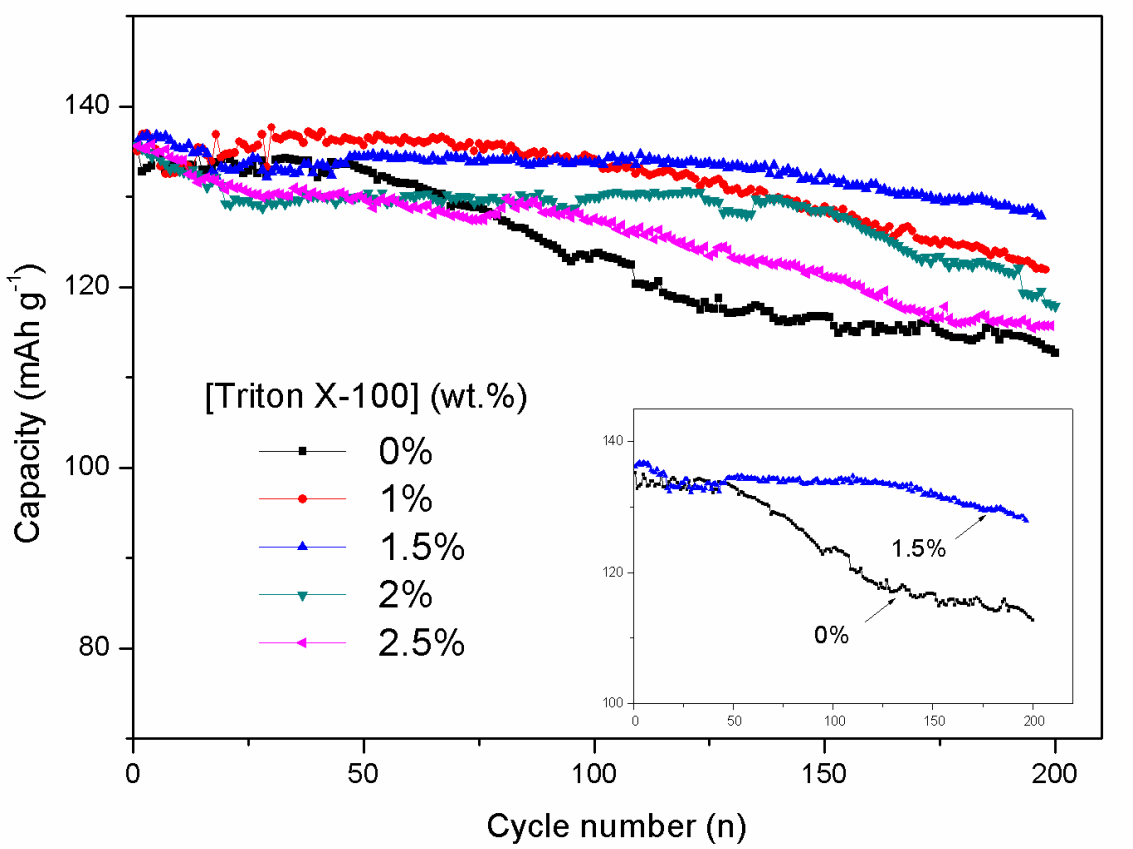


**Figure 2.** Cycle performance of cathodes with different Triton X-100 contents at 1 C between 2.5 V and 4.2 V. The inset figure shows the comparison of $LiFePO_4$/SP cathode and $LiFePO_4$/SP-T cathode containing 1.5 wt.% of Triton X-100

The rate capability of $LiFePO_4$/SP cathodes with various Triton X-100 contents is shown in Fig. 3. The electrodes have the similar discharge capacities at 0.1 C. However, with the increase of discharge–charge current rate, electrochemical performance of the electrode are influenced by the contents of Triton X-100, i.e. the discharge capacity increases until 1.5 wt.% of Triton X-100. The discharge capacity for $LiFePO_4$/SP-T cathode containing 1.5 wt.% of Triton X-100 is 101 mAh $g^{-1}$ but $LiFePO_4$/SP cathode is 88 mAh $g^{-1}$ at 4 C. Compared with the $LiFePO_4$/SP cathode, $LiFePO_4$/SP-T cathodes show a better discharge capacity, especially in the case of high rate. It is likely that the variation of the discharge capacity for these electrodes is due to the difference in the electronic wiring of the active particles. The improvement of rate capability for $LiFePO_4$/SP-T cathodes can be attributed to that the SP is more homogeneously dispersed, improving the electrical contact between the SP and $LiFePO_4$ nano-particles and can obtain the lower potential polarization of the cathode during the charge and discharge processes.

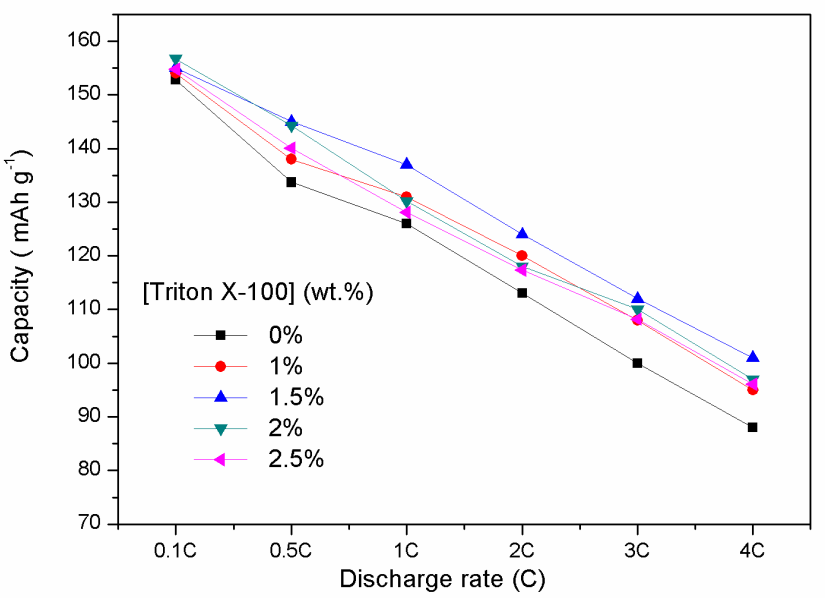


**Figure 3.** Rate capability of cathodes with different Triton X-100 contents at 0.1~4 C

To better characterize the capacity fading mechanisms of the $LiFePO_4$ cathodes, EIS method was used for measuring the cell containing the $LiFePO_4$ cathode, which can help to clarify the ohmic resistance and polarization resistance behaviors coincident with capacity loss. Fig. 4 shows Nyquist plots obtained from the $LiFePO_4$/SP-T and the $LiFePO_4$/SP cells after 200 cycles test. The impedances of the cells after cycle test were measured at a fully charged state and analyzed by Zview software. In general, a high frequency pronounced semicircle is related to the resistance of charge transfer reaction resistance ($R_{ct}$), which represents the charge transfer capacity in the electrode [21-22]. It can be seen from Fig. 4 that the $R_{ct}$ of $LiFePO_4$/SP cell is maximum. $R_{ct}$ of $LiFePO_4$/SP-T cells reduced significantly and with Triton X-100 concentrations increased, $R_{ct}$ of $LiFePO_4$/SP-T cells was decreased firstly then increased, which Triton X-100 content corresponds to 1.5% is minimum. This variation trend of EIS is consistent with the cycle performances of cells in Fig. 3.

The change in impedance is a main factor which affects the cycling and rate performance of batteries. After adding the right amount of Triton X-100, the agglomeration of SP has been improved. The SP could be dispersed in the surrounding of the $LiFePO_4$ particles uniformly to form good conductive channels, so that reduced the polarization of battery during the charge and discharge processes, thus the reversibility of battery and electrochemical performances are improved. However, when adding too more Triton X-100, the dispersants were adsorbed on the SP surface and their tail-end long chain would produce a "bridged" phenomenon. That could cause soft agglomeration of the SP particles. And the insulativity of Triton X-100 may reduce the charge transfer capability of the SP and $LiFePO_4$ particles, which lead to the impedance increased. Therefore, the trend of $R_{ct}$ was decreases firstly and then increases. Based on the above data, the electrochemical performance of the cells when the cathode containing 1.5 wt.% of Triton X-100 is best. So that we mainly compared the difference between these two samples ($LiFePO_4$/SP and $LiFePO_4$/SP-T containing 1.5 wt.% of Triton X-100) in the following article.

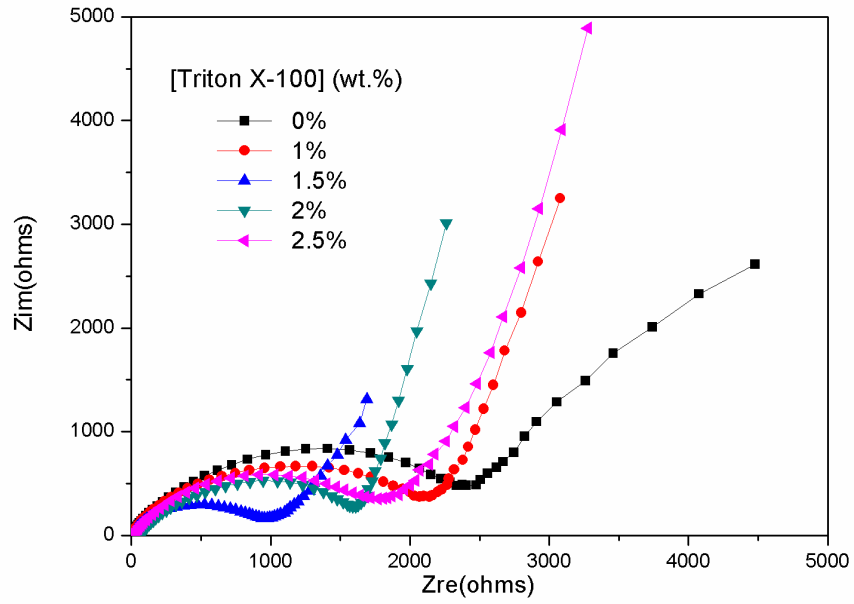


**Figure 4.** A. C. impedance plots of cathodes with different Triton X-100 contents after 200 cycles

The cyclic voltammograms of the $LiFePO_4$/SP and $LiFePO_4$/SP-T cathode containing 1.5 wt.% of Triton X-100 are shown in Fig. 5, respectively. A pair of redox peaks appears in the CV curves is typical redox peaks of $LiFePO_4$ electrode [23]. It is clear that the oxidation peaks of $LiFePO_4$/SP-T cathode shift to the left, the reduction peaks shift to the right, the voltage difference between the redox peaks decrease from 0.486 V to 0.360 V, and the redox peaks are much sharper than that of the $LiFePO_4$/SP cathode. These confirm that the redox reaction rate of the $LiFePO_4$/SP-T cathode is faster, and indicates the weakening of polarization in the cell, better kinetics characteristics and better reversibility of $LiFePO_4$/SP-T cathode. Since both cathodes are fabricated identically except for the inclusion of Triton X-100, this confirms that by using Triton X-100 during cathode fabrication improves the dispersion of the SP, presumably because the electron transfer rate is increased by more uniform conductive channels. The curves of sweeps 1 and 2 for the $LiFePO_4$/SP-T cathode are very similar in shape. It should be noted that the dispersant Triton X-100 is electrochemically stable over the 2.5-4.5 V voltage range.

The effect of Triton X-100 on SP dispersion is investigated further by scanning electron microscopy imaging of the $LiFePO_4$ cathode surface. Fig. 6 (a) and (b) show microstructures of the top surfaces of $LiFePO_4$ electrode prepared with SP and SP-T, respectively. It is obvious that SP formed heavy agglomeration itself, which cannot be well scattered on the $LiFePO_4$ surface to form an effective contact in Fig. 6 (a). In contrast, the Fig. 6 (b) shows the $LiFePO_4$ cathode prepared with SP-T is seen to possess better uniformity and smaller particle size of SP-T surrounding the $LiFePO_4$ particles which suggests an improved electrical contact between the SP-T and $LiFePO_4$ particles. Compared to the cathode with SP, the particles of the cathode with SP-T could form the better conductive channels that weakening the polarization. So the rate capability of the battery could be enhanced.

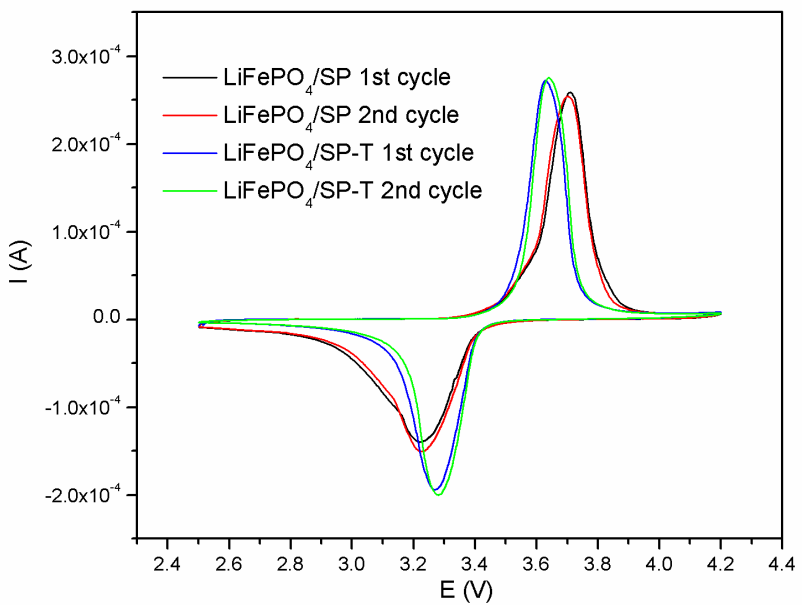


**Figure 5.** Cyclic voltammograms of $LiFePO_4$/SP and $LiFePO_4$/SP-T cathodes containing 1.5% Triton X-100: Sweep rate is 0.1 $mV \cdot s^{-1}$.

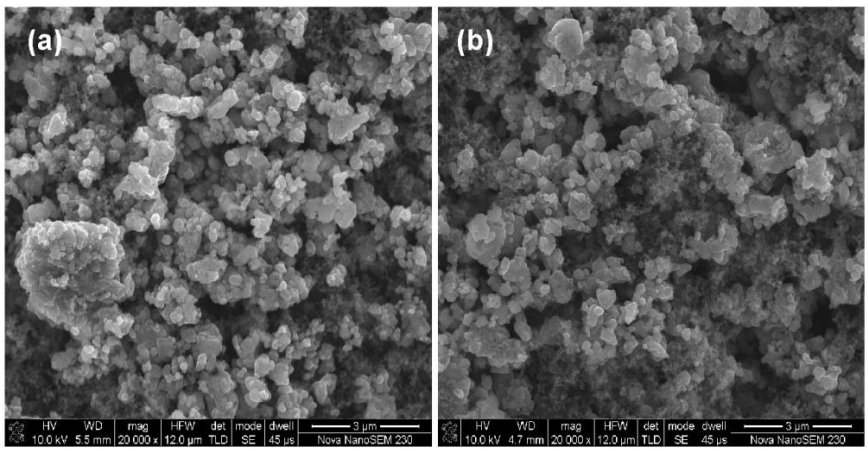


**Figure 6.** SEM images of different $LiFePO_4$ cathodes before charge, (a) $LiFePO_4$/SP and (b) $LiFePO_4$/SP-T containing 1.5% Triton X-100

*3.2 Triton X-100 dispersion effect tests*

Particle size distribution of SP and SP-T in the NMP solvent was measured in order to evaluate their agglomeration state, and the results were shown in Fig. 7. We can see that the SP apparent particle size in the NMP solution (D50) is about 12.12 μm, larger than that of SP-T (6.60 μm). In both cases, the suspended SP particles are quite larger than the initial 40 nm of the as-supplied SP powder, demonstrating a basic flocculation tendency of the NMP-suspended SP particulates because the poor compatibility between hydrophobic carbon black and NMP (polar energy ~12.3 $MPa^{1/2}$) [24]. But the particle size of SP-T is significantly smaller than the SP, besides the particle size distribution is significantly narrower, which indicate that the particle size is more uniform. Particle size and

distribution are affected by the dispersion properties of SP in NMP. Well-dispersed SP results in the particle size distributions of SP shift to the left, i.e., toward smaller particle diameters. Improvement of the SP-T dispersion in the electrode slurries results in more homogeneous SP distribution within the dried composite electrode and better electronic wiring of the active material particles, leading to higher discharge capacity at high rates.

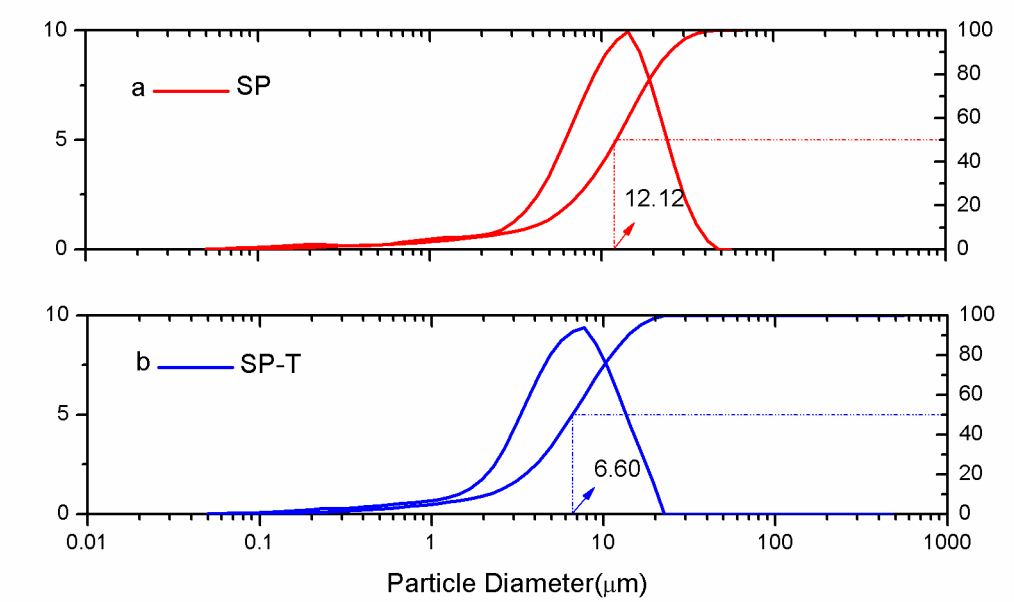


**Figure 7.** Particle size distribution of carbon black

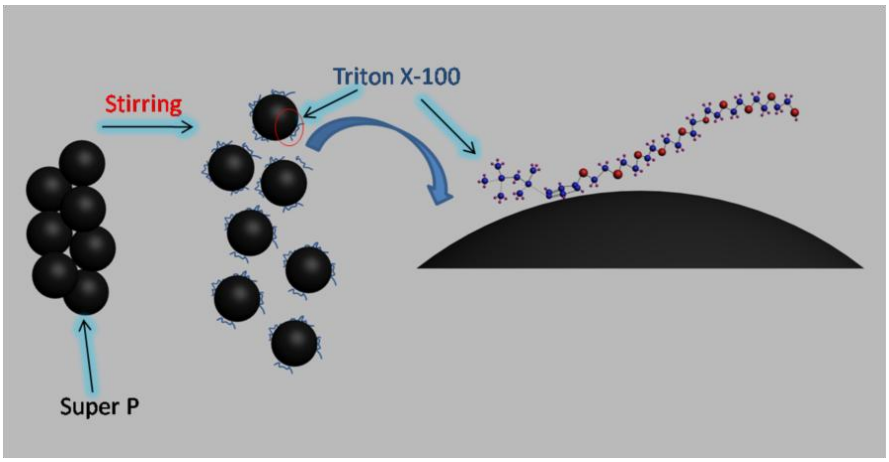


**Figure 8.** Schematic illustration of dispersion principle

These improved dispersion properties of SP-T originate from Triton X-100 has a favorable conformation for dispersion of particles due to steric effects. The isooctyl chain on the benzene ring could be adsorbed on SP, whereas the benzene ring contributes greatly to the adsorption to the graphitic surface because of π-π stacking type interaction [11, 19]. The lyophilic group (PEO) facing

toward the medium provides effective steric stabilization to overcome the large van der Waals forces among the SP particles, thereby improving the dispersion effect of SP. Schematic illustration of dispersion principle is present in Fig. 8.

Rheological behavior of SP suspension and SP-T suspension (SP: Triton X-100 is 20: 3) were characterized, and the results are shown in Fig. 9. All suspensions show shear thinning behaviors, showing linear dependence of the viscosity on the shear rate, i.e. a decrease of the viscosity with increasing shear rate. This is typical of flocculated dispersions where the presence of weak attractive forces between the particles leads to the formation of clusters of particles. It is also noticeable that the addition of Triton X-100 significantly decreased the viscosity of the SP-T suspension, which resulted from the improvement of dispersion properties of SP-T. This is well-consistent with the results for particle size distribution (Fig. 7). Therefore, it is clear that the addition of Triton X-100 contributes to the improvement of dispersion properties of SP-T through steric stabilization.

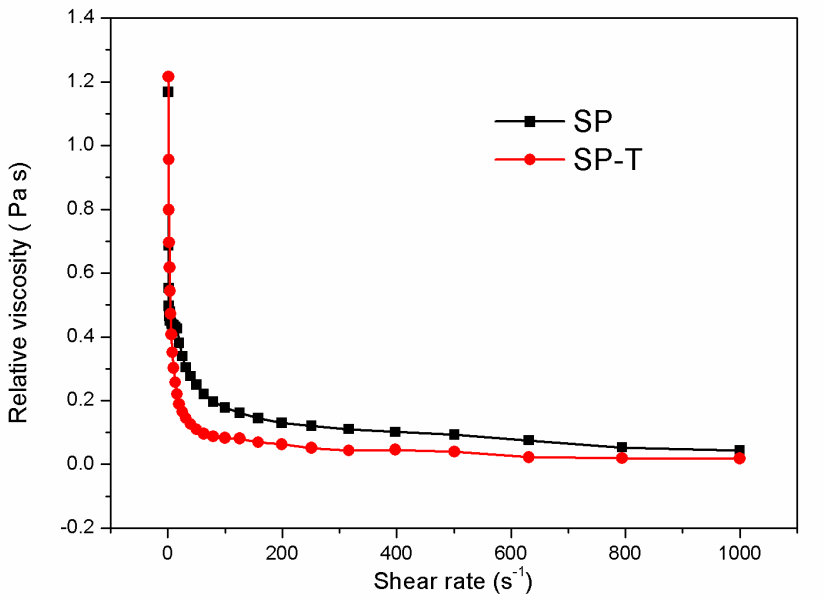


**Figure 9.** Relative viscosity as a function of shear rate for SP and SP-T (SP: Triton X-100 is 20: 3)

## 4. CONCLUSIONS

In this paper, we have clearly demonstrated that nano-conductive carbon agent can be pre-dispersed with Triton X-100 as dispersant in organic N-methyl-pyrrolidone (NMP) solvent system and the dispersion properties of nano-conductive carbon agent have a great impact on the electrochemical performance of the electrodes

When the $LiFePO_4$/SP-T cathode containing 1.5 wt.% of Triton X-100, the SP-T had a narrower size range than SP and the $LiFePO_4$/ SP-T cathode has more homogeneous microstructures compared to the $LiFePO_4$/SP cathode. Improvement of the SP-T dispersion in the electrode slurries

results in more homogeneous SP-T distribution within the dried composite electrode and better electronic wiring of the active material particles, leading to better electrochemical performance.

A dispersant is needed to disperse the nano-conductive carbon agent (SP) and obtain a satisfactory suspension processing of a $LiFePO_4$ composite electrode for lithium ion battery. The poly (ethylene glycol) p-isooctyl-phenyl ether (Triton X-100) is an efficient non-ionic surfactant which can be used for the purpose. We believe that such methodology will have certain advantage for the development of the lithium ion battery technology in the future. Our future work will continue to explore alternative formulae for Triton X-100, as well as various combinations of alternative SP materials.

ACKNOWLEDGMENTS
The authors thank the financial support of the National Key Technology Research and Development Program of China (2007BAE12B01) and the National Natural Science Foundation of China (20803095). We also thank the support of the Engineering Research Center of Advanced Battery Materials, the Ministry of Education, China.

**References**

1. Y. Wang, P. He, H. Zhou, *Energy Environ. Sci.*, 4 (2011) 805.
2. Y. Ma, X. L. Li, S. F. Sun, X. P. Hao, Y. Z. Wu, *Int. J. Electrochem. Sci.*, 8 (2013) 2842
3. K. Wang, Y. Wu, S. Luo, X. F. He, J. P. Wang, K. L. Jiang, S. S. Fan, *Journal of Power Sources*, 233 (2013) 209.
4. R. Dominko, M. Gaberscek, J. Drofenik, M. Bele, S. Pejovnik, J. Jamnik, *J. Power Sources*, 149 (2002) A1598.
5. Z. Liu, J.Y. Lee, H. Lindner, *J. Power Sources*, 97 (2001) 361.
6. A. Varzi, C. Täubert, M. Wohlfahrt-Mehrens, M. Kreis, W. Schütz, *J. Power Sources*, 196 (2011) 3303.
7. M. E. Spahr, D. Goers, A. Leone, S. Stallone, Eusebiu. Grivei, *J. Power Sources*, 196 (2011) 3404.
8. K.C. Ruthiya, J. van der Schaaf, B.F.M. Kuster, J.C. Schouten, *Chem. Eng. Sci.*, 60 (2005) 6492.
9. S. Kuroda, N. Tobori, M. Sakuraba, Y. Sato, *J. Power Sources*, 119 (2003) 924.
10. E. Ligneel, B. Lestriez, O. Richard, D. Guyomard, *J. Phys. Chem. Solids*, 67 (2006) 1275.
11. B. Wu, L. Bai, Q. M.Gong, J. Liang, *Acta Phy. -Chim. Sin.*, 25 (2007) 1605.
12. N. Faouzi, A. Naceur, C. Yves, *Progress in Organic Coatings*, 55 (2006) 303.
13. A. Tomlinson, B. Scherer, E. Karakosta, M. Oakey, T.N. Danks, D.M. Heyes, S. E. Taylor, *Carbon*, 38 (2000) 13.
14. F. M. Smiechowski, V. F. Lvovichb, *Journal of Electroanalytical Chemistry*, 577 (2005) 67.
15. J. Kima, B. Kim, J. Lee, J. Cho, B. Park, *Journal of Power Sources*, 139 (2005) 289.
16. W. Porcher, B. Lestriez, S. Jouanneau, D. Guyomard, *Journal of Power Sources* 195 (2010) 2835.
17. P. Ping, Q. Wang, J. Sun, H. Xiang, C. Chen, *J. Electrochem. Soc.*, 157 (2010) A1170.
18. C. C. Chang, L. J. Her, H. K. Su, S. H. Hsu, Y. T. Yen, *J. Electrochem. Soc.*, 158 (2011) A481.
19. C. M. Gonzalez-Garcia, M. L. Gonzalez-Martin, V. Gomez-Serrano, J. M. Bruque, L. Labajos-Broncano, *Langmuir*, 16 (2000) 3950.
20. G. L. Yang, A. F. Jalbout, Y. Xu, H. Y. Yu, X. G. He, H. M. Xie, *Electrochem. Solid-State Lett.*, 11 (2008) A125.
21. J. Li, C. F. Yuan, Z. H. Guo, Z. A. Zhang, Y. Q. Lai, J. Liu, *Electrochim. Acta*,, 65 (2012) 69.

22. P. L. Moss, G. Au, Plichta, E. J. Plichta, Zheng, J. P. Zheng, *J. Power Sources*, 189 (2009) 66.
23. Y. W. Chen, J. S. Chen, *Int. J. Electrochem. Sci.*, 7 (2012) 8128.
24. J. H. Lee, S. B. Wee, M. S. Kwon, H. H. Kim, J. M. Choib, M. S. Song, H. B. Park, H. Kim, U. Paik, *J. Power Sources*, 196 (2011) 6449.